Thermography at Millimetre Wavelengths for Security Inspection of Footwear

Stuart W. Harmer[1, *], Christopher I. Johnson[2], Dana Wheeler[3], and Hashim Bhabha[1]

Abstract—Millimetre-wave thermography is used to image through the soles of shoes as proof of principle study into the application of such an approach for security inspection. Current airport security screening practice necessitates the removal of shoes prior to x-ray screening for potential threats or other concealments, for example explosive or explosive precursor materials; narcotic substances or small weapons. The authors demonstrate that thermography at ~ 250 GHz is able to reveal a variety of objects concealed within the soles of typical shoes, and that such an approach might be applied to rapidly screen passengers without necessitating the removal of their footwear.

1. INTRODUCTION

Imaging in the microwave (0.3–30 GHz) and millimetre-wave (30–300 GHz) bands of the electromagnetic spectrum is an accepted and well understood security screening tool, which is most commonly encountered at airports [1–3]. Imaging systems operating at the higher end of the microwave band and across the millimetre wave band are well suited to this application, due to a combination of optimal electromagnetic material properties of typical clothing; acceptable physical limitations on system size; imaging performance; cost and human safety [4]. Imaging in the microwave and millimetre-wave band can be 'passive' or 'active', depending on whether the images are formed by thermal emission only (thermography) or by illumination of the imaged area with electromagnetic radiation in the appropriate band (active). Active systems are further categorized by whether the illuminating radiation is coherent or incoherent in nature. There are many examples in the literature discussing various aspects of the application of microwave and millimetre-wave imaging for security screening of people and a wide range of other remote sensing applications [5–10].

Since 2001, screening of passengers' footwear at airport security checkpoints has been in force. Due to design, currently deployed microwave and millimetre-wave screening systems are unable to carry out screening of footwear simultaneously with screening of the limbs and torso. In fact, at the time of writing, there are no commercially available footwear screening systems operating in the microwave or millimetre-wave bands. Currently, passengers remove their shoes and these are then screened, predominantly with x-ray computer tomography (CT) systems, for materials such as explosives [11]. The removal and subsequent replacement of footwear at airport security checkpoints is a source of considerable delay and inconvenience to passengers, which could be mitigated to some extent by a screening process that does not necessitate the removal of footwear.

The materials, from which shoes are constructed, leather, rubber, plastics, etc., generally have complex permittivity values which permit propagation of electromagnetic waves in the microwave or millimetre-wave region of the electromagnetic spectrum with acceptable loss [12] and thus a similar

[1] Department of Engineering & Design, University of Chichester, College Ln, Chichester, W. Sussex PO19 6PE, UK. [2] Department of Electrical Engineering, Manchester Metropolitan University, John Dalton Building, Chester Street, Manchester M1 5GD, USA. [3] Plymouth Rock Technologies Inc., Plymouth Rock Technologies, 202 South Meadow Road, Unit 5, Plymouth, MA 02360, USA.

approach as for body and limb screening may be taken to reveal objects concealed within footwear. Objects and materials of potential interest include, explosive substances or their precursors; narcotics; weapons (bladed or small firearms); and currency.

2. THEORETICAL DISCUSSION

Thermography (passive imaging), at microwave and millimetre-wave bands relies on differences in brightness temperature in the scene to provide contrast [13]. Objects at room temperature $\sim 300\,\text{K}$, emit in the microwave and millimetre-wave band with intensity depending linearly on the product of their temperature and emissivity. The spectral radiance, β, in the regime where the photon energy is much smaller than the product of Boltzmann's constant with temperature, $kT \gg hv$, is given by Eq. (1)

$$\beta \approx \frac{2v^2 kT}{c^2} \tag{1}$$

Hence, the power emitted, dP in the frequency band $d\nu$, from an area ds, at temperature T and with emissivity η, in the direction θ from the normal of the emitting surface and into the solid angle $d\Omega$, is given by Eq. (2)

$$dP = \frac{2v^2 kT}{c^2} \eta \cos\theta d\Omega ds d\nu \tag{2}$$

Consider an imaging system which is sensitive to radiation in the band ν to $\nu + \Delta v$ (assuming, $\Delta v \ll \nu$) and which intercepts, by virtue of its principal aperture, the radiation emitted into a solid angle Ω. The power received by the system from an area ds in the scene is, therefore, given by Eq. (3)

$$dP \approx \alpha T \eta ds \tag{3}$$

where for brevity we have used $\alpha = \frac{2\nu^2 k \Delta v}{c^2} \int_{\Omega} \cos\theta d\Omega$ and assumed constant emissivity over the bandwidth of the system. The quantity, $U = \eta T$, is the brightness temperature. By applying standard paraxial imaging theory [14], we may relate the spatial distribution of the brightness temperature in the scene, U, and image U' as,

$$U' = U \otimes \rho + \Delta U \tag{4}$$

where ρ is the point spread function of the imaging system; $\otimes$ represents the two-dimensional convolution operation; and U has been scaled according to the magnification of the imaging system. The term ΔU in Eq. (4) represents a normally distributed random variable with expectation value of zero and standard deviation equal to the noise equivalent temperature difference (NETD) of the imaging system. The NETD of the system depends primarily on the characteristics of the initial amplification stage of the system and some other system parameters [15]. NETD is an important figure of merit for a passive millimetre-wave imaging system and limits the system's sensitivity to brightness temperature differences. The contrast in the image is due to spatial variations in both temperature and emissivity. Such an image is sometimes referred to as a thermograph and the technique of thermography is more commonly implemented at infra-red wavelengths for a variety of remote sensing applications [16].

Objects in the scene may not only emit radiation in the microwave and millimetre band according to Eq. (2), they may also reflect and transmit such radiation from other sources. The relation between the emissivity (absorptance), η, reflectance, r, and transmittance, t, of a surface in the scene is given by Eq. (5)

$$\eta + r + t = 1 \tag{5}$$

We consider a simple three-layer system as representative of a worn shoe, see Figure 1. Hence, the brightness temperature recorded by an imaging system working in the microwave or millimetre-wave bands would be,

$$U' = (rT_3 + \eta T_2 + tT_1) \otimes \rho + \Delta U \tag{6}$$

where η, r, and t describe the emissivity, reflectance, and transmittance of the three-layer system. Note, it follows immediately from Eq. (5) and Eq. (6), that if all three regions are at the same temperature, $(T_1 = T_2 = T_3)$ then the brightness temperature is constant and the contrast in the thermograph will be
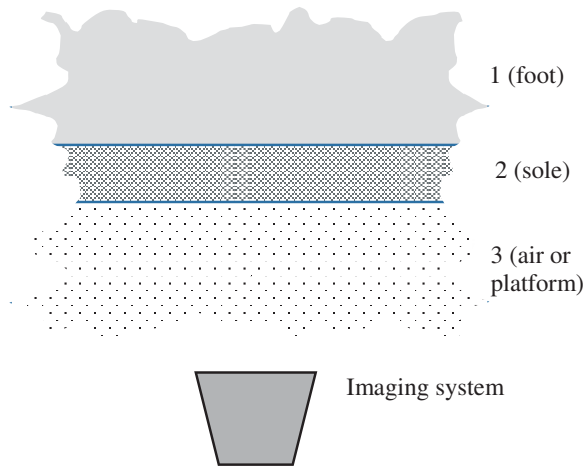
Figure 1. Three-layer system representing a simplistic shoe: layer 1 is the foot; layer 2 the sole of the shoe and layer 3 air or some suitably microwave transparent material upon which the wearer stands.

Figure 2. Running type shoe; modified for concealment (left) and unmodified (right); concealments of putty, wax, sugar (wrapped) and scissors used are shown.

associated solely with system noise. We choose, arbitrarily, to work with the reflectance and emissivity, hence from Eqs. (5) and (6) we obtain Eq. (7),

$$U' = (T_1 + r(T_3 - T_1) + \eta(T_2 - T_1)) \otimes \rho + \Delta U \tag{7}$$

To provide contrast, one must arrange to have temperature differences between regions which are significantly greater than the NETD of the system ($\sim 1\,\mathrm{K}$).

3. EXPERIMENTAL CONFIGURATION

For thermographic inspection, a modified commercial millimetre wave imaging system was used; this system operates at a centre frequency of $\sim 250\,\mathrm{GHz}$ and has a $175\,\mathrm{mm}$ diameter primary aperture, a focal length of $1\,\mathrm{m}$, and an NETD $\sim 1.0\,\mathrm{K}$. The system provides collocated imagery in the visible and millimetre-wave bands and operates at 6 frames per second in the millimetre-wave band, providing an image with 240 by 140 pixels. The system used is a modified version of the Thruvision TS4 commercial millimtre-wave imaging system, which is sold for the applications of security screening of people and for theft prevention. In the system discussed in this paper, the reflector curvature has been altered to move the focal distance from infinity to a distance of $\sim 1\,\mathrm{m}$, which provides higher spatial resolution ($\sim 1\,\mathrm{cm}$) images of small regions, such as the soles of shoes. The TS4 uses four receivers based on GaAs Schottky mixers and scans the scene over these receivers using a lightweight oscillating reflector.

A pair of used, running shoes served as one sample to test and some loafer type shoes as a second sample. One shoe from each sample was modified by removal a small approximately square portion of the midsole and filled with one of three simulated explosiveor narcotic materials: putty; wax and sugar. Once the substance has been placed in the shoe, the lower portion of the excavated midsole is replaced, rendering the concealment nearly invisible to the human eye. Additionally, a pair of scissors was placed within the shoe, under the insole, to simulate the concealment of a bladed weapon. See Figure 2. To provide contrast, a flexible gel pack was heated in water to $\sim 35\,\mathrm{C}$ and inserted into the shoe with the surface in contact with the entire insole of the shoe. To ensure that thermal equilibrium is approximately reached in the sample, multiple gel packs were used and replaced every ~ 1 minute for 10 minutes prior to imaging. Images taken after application heat for only 1 minute show increased contrast due to the larger temperature differences in the shoe; after several minutes of heat application, images are largely

unchanging with time and so thermal equilibrium can be assumed to be reached. Some effects relating to the longer heating time of the denser rubber soled loafer show were noted and are noted in Section 4. Measurements took place within and indoor laboratory with a controlled air temperature of ~ 18 C. The presence of a concealment is made by direct visual comparison of the millimetre-wave thermographs of modified and unmodified shoes from the same sample. Where there is a clear difference between the two thermographs and where the thermograph of the modified shoe shows an area which is obviously correlated with the concealed object, then this is considered a 'detection'.

Example thermographs captured with the system are shown in Figure 3. The human hand, shows positive contrast (white) to the background (black) because the hand and arm have a higher brightness temperature; human skin has an emissivity of ~ 0.8 at 250 GHz [6] and hence, assuming the laboratory walls emit as a black body at a temperature of 291 K and with the skin at 303 K, we would expect a positive contrast of $\sim (303-291) \times 0.8 \sim 10$ K between hand and background. The system automatically adjusts the dynamic range of the image according to the highest and lowest brightness temperatures within the scene, so the presence of noise in the image of the hand and arm is clearly visible as light and dark regions in the background of the image as would expected with an NETD ~ 1 K. The ceramic cup contains water at ~ 80 C (353 K) and behaves as a near blackbody object and hence, we would expect a positive contrast of ~ 60 K between cup and background. Brightness temperature variations due to noise in the background are no longer visible due to the much higher contrast that this target presents; contrast is some 60 times the NETD. In the image with the human hand partially obscuring the cup, we can see that the hand has a negative contrast relative to the cup; we would estimate a negative contrast of ~ 50 K between hand and cup and a positive contrast of ~ 10 K between hand and background.
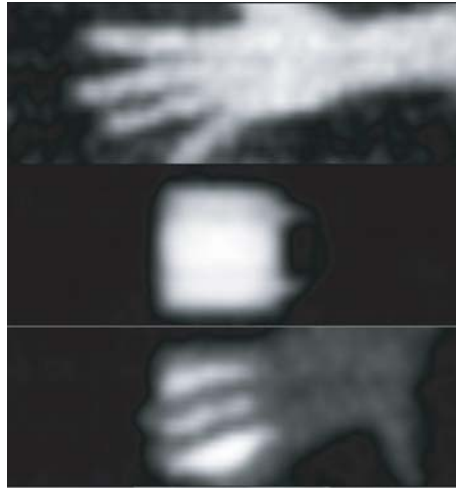

Figure 3. Example of thermographic images captured with the apparatus described. Top, a human hand; Middle, a ceramic cup of hot liquid; Bottom, a human hand partially obscuring a cup of hot liquid.

4. RESULTS

The results are somewhat subjective in that they rely on human interpretation of captured images, i.e., whether the shoe with the concealment can be easily differentiated from the image of the unmodified shoe by visual inspection of the thermograph. In a commercial system, such interpretation would likely be undertaken by application of an automated threat detection algorithm, based on one or more image processing techniques [17]. Selected thermographs are presented in Figure 4. and the results of inspection of all thermographs is detailed in Table 1.

In all cases, the limited number of concealed objects could be detected and correlated with their position within the shoe. The running shoe has soles 10–20 mm in thickness and some internal structure of the sole is visible in the central and heel regions of the shoe in the thermographic image, see Figure 4.
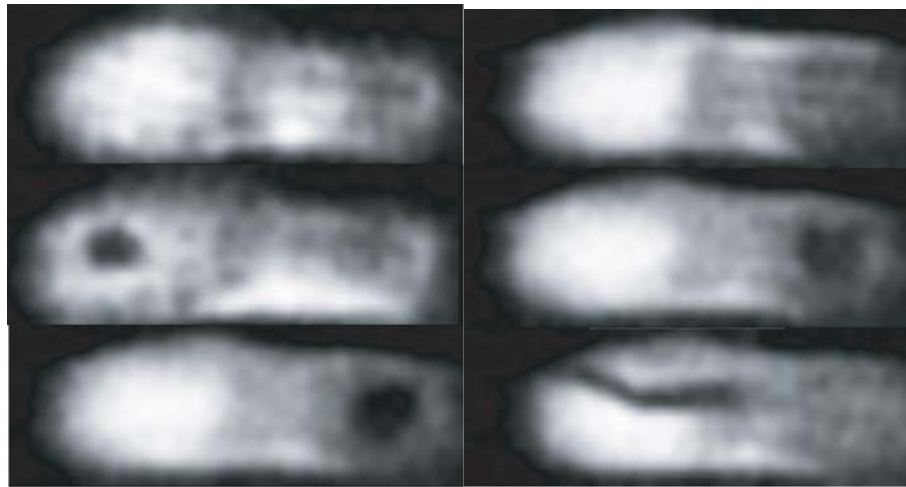
Figure 4. Thermographic images of shoe with and without concealed objects; Top Left, training shoe with no concealments; Middle Left, Training shoe with a coin placed under insole in the toe area of the shoe; Bottom Left, loafer shoe with ∼ 10 g of sugar placed within heel section of shoe; Top Right, loafer shoe with no concealments; Middle Right, loafer shoe with ∼ 10 g of putty placed in the heel area of the shoe; Bottom Right, loafer shoe with scissors placed under insole of shoe. The toe areas of the shoe are in the left hand side of each image.

Table 1. Detection of concealments.

Sample	Concealment	Comments
Running shoe	Putty	This target produces a negative contrast and is easily identifiable within the thermographic image
Running shoe	Sugar	This target produces a negative contrast and is easily identifiable within the thermographic image, see Figure 4.
Running shoe	Wax	This target is harder to identify than Putty or sugar and produces a positive contrast within the thermographic image.
Running shoe	Scissors	This target produces a negative contrast and the bladed section is easily identifiable.
Running shoe	Unmodified	The shoe shows some contrast, particularly in the middle and heel sections of the shoe. See Figure 4.
Loafer	Putty	This target is identifiable in the heel section of the shoe, displaying a negative contrast in the thermographic image. See Figure 4.
Loafer	Sugar	This target is identifiable in the heel section of the shoe, displaying a negative contrast in the thermographic image. See Figure 4.
Loafer	Wax	This target is identifiable by in the heel of the shoe, producing a positive contrast within the thermographic image.
Loafer	Scissors	This target produces a negative contrast and the bladed section is easily identifiable, see Figure 4.
Loafer	Unmodified	The shoe shoes distinct contrast between the toe and heel sections of the shoe. See Figure 4.

A 10 pence coin placed under the insole in the toe region for the running shoe is easily visible, displaying a strong negative contrast as would be expected, see Figure 4. The loafer shoe has a denser sole than that of the running shoe and displays a higher emissivity. This fact was notable in the time taken for the contrast in the thermograph of the loafer to maximize. In the case of the running shoe, the

temperature of the sole plays only a small part in the contrast mechanism as the material has low loss, hence the emissivity term in Eq. (7) may be reasonably neglected and heating of the sole has minimal effect on the thermograph contrast. The loafer sole has a significant emissivity and begins, when the heated gel pack is first inserted, with $T_2 \sim T_3$, as the sole heats, $T_2 > T_3$, and according to Eq. (7) the contrast between shoe and background increases. Multiple gel packs were heated and replaced to achieve an approximate thermal equilibrium within the test shoes before images were captured. The loafer without modification, see Figure 4, shows the effect of the thicker lossy sole of this shoe with a significant contrast between the toe and heel areas of the shoe. The sugar, wrapped in plastic film, and placed within the excavated heel section of the loafer is clearly visible, see bottom image of Figure 4. The putty also provides a strong negative contrast when being concealed in the heel section of the loafer, see Figure 4. Scissors, with a distinctive angled blade design n, see Figure 2, are clearly visible when being concealed within the shoe, under the loafer shoe's removable insole, see Figure 4.

5. CONCLUSION

The results from this study show that thermography at millimetre-wavelengths has the capability to provide a safe and rapid screening method for inspecting air passengers' footwear. The proposed technique could be used as a pre-screening method, which may reduce the number of passengers who are required to remove their shoes and place these into the standard x-ray CT imaging machines. Improvements in results are likely to be obtained if a heated element is used to increase temperature contrast in the thermographic images. The results also show that shoe soles are typically relatively transparent at millimetre-wave frequencies and that an active imaging approach [18] might also be used for the same application.

REFERENCES

1. Appleby, R. and R. N. Anderton, "Millimeter-wave and submillimeter-wave imaging for security and surveillance," *Proceedings of the IEEE*, Vol. 95, No. 8, 1683–1689, Aug. 2007.
2. Appleby, R. and H. B. Wallace, "Standoff detection of weapons and contraband in the 100 GHz to 1 THz region," *IEEE Transactions on Antennas and Propagation*, Vol. 55, 2944–2956, 2007.
3. Kemp, M. C., "Millimetre wave and terahertz technology for the detection of concealed threats — A review," *Proceedings of SPIE*, Vol. 6402, 2006.
4. Agurto, A., Y. Li, G. Tian, N. Bowring, and S. Lockwood, "A review of concealed weapon detection and research in perspective," *Proc. IEEE Int. Conf. MonE02 Networking, Sensing and Control*, 443–448, 2007.
5. Salmon, N. A., "W-band real-time passive millimeter-wave imager for helicopter collision avoidance," *Proc. SPIE*, Vol. 3703, 28–32, Apr. 1999.
6. Owda, A. Y., N. Salmon, S. W. Harmer, S. Shylo, N. J. Bowring, N. D. Rezgui, and M. Shah, "Millimeter-wave emissivity as a metric for the non-contact diagnosis of human skin conditions," *Bioelectromagnetics*, Vol. 38, 559–569, 2017.
7. Harmer, S. W., S. Shylo, M. Shah, N. J. Bowring, and A. Y. Owda, "On the feasibility of assessing burn wound healing without removal of dressings using radiometric millimetre-wave sensing," *Progress In Electromagnetics Research M*, Vol. 45, 173–183, 2016.
8. Mann, C., "First demonstration of a vehicle mounted 250 GHz real time passive images," *Proc. SPIE*, Vol. 7311, 73110Q-1–73110Q-7, May 2009.
9. Appleby, R., P. Coward, and J. N. Sanders-Reed, "Evaluation of a passive millimeter wave (PMMW) imager for wire detection in degraded visual conditions," *Proc. SPIE*, Vol. 7309, 73090A-1–73090A-8, Apr. 2009.
10. Waldschmid, C., E. Topak, J. Hasch, R. Schnabel, R. Weigel, and T. Zwick, "Millimeter-wave technology for automotive radar sensors in the 77 GHz frequency band," *IEEE Transactions on Microwave Theory and Techniques*, Vol. 60, No. 3, 845–860, Mar. 2012.

11. Singh, S., "Explosives detection systems (EDS) for aviation security," *Signal Processing*, Vol. 83, No. 1, 31–55, 2003.

12. Lamb, J. W., "Miscellaneous data on materials for millimetre and submillimetre optics," *International Journal of Infrared and Millimeter Waves*, Vol. 17, No. 12, 1997–2034, Dec. 1996.

13. Yujiri, L., M. Shoucri, and P. Moffa, "Passive millimeter-wave imaging," *IEEE Microwave Magazine*, Vol. 4, No. 3, 39–50, 2003.

14. Goodman, J. W., *Introduction to Fourier Optics*, McGraw Hill, Jan. 2005.

15. Sinclair, G. N., R. N. Anderton, and R. Appleby, "Outdoor passive millimetre wave security screening," *Proc. IEEE 35 Annual 2001 International Carnahan Conference on Security Technology*, Oct. 2001.

16. Prasad, B. S., K. A. Prabha, and P. V. S. G. Kumar, "Condition monitoring of turning process using infrared thermography technique — An experimental approach," *Infrared Phys. Technol.*, Vol. 81, 137–147, Mar. 2015.

17. Dietlein, C. R., E. Grossman, F. G. Meyer, X. Shen, and Z. Popovic, "Detection and segmentation of concealed objects in terahertz images," *IEEE Transactions on Image Processing*, Vol. 17, No. 12, Dec. 2008.

18. Andrews, D. A., D. O'Reilly, M. J. Southgate, N. D. Rezgui, N. J. Bowring, and S. W. Harmer, "Development of an ultra-wide band microwave radar-based footwear scanning system," *Proc. SPIE Security + Defence*, Vol. 8900, Oct. 2013.